International Journal of Nanoelectronics and Materials
IJNeaM
ISSN 1985-5761 | E-ISSN 2232-1535

Improving Cellular Behaviour of Low Modulus Ti-Alloy by Controlling Anodizing Parameter

Tukur Tsauri Bashir[a,b], Hussain Zuhailawati[a*], Lockman Zainovia[a] and Mohamed Abdel-Hady Gepreel[c]

[a]*School of Materials and Mineral Resources Engineering, Universiti Sains Malaysia (USM), 14300 Nibong Tebal, Pulau Pinang, Malaysia*
[b]*Department of Welding and Fabrication Engineering Technology, Hassan Usman Katsina Polytechnic (HUKPOLY), P.M.B. 2052 Katsina, Nigeria*
[c]*Department of Materials Science and Engineering, Egypt-Japan University of Science and Technology (E-JUST), New Borg El-Arab City, Alexandria 21934, Egypt*
**Corresponding author. Tel.: +60-1642-1200-1; e-mail: zuhaila@usm.my*

ABSTRACT

The behaviour of biomaterial is widely related to its surface characteristics. Studies indicated that rough surfaces enjoy more clinical success and display more bioactivity than their polished counterparts. In line with this and the commanding effect the anodization parameters have on the overall surface roughness, the effects of the anodization parameter on bioactivity of low modulus Ti-13Mo-2Fe were investigated. Two electrodes in fluoride based organic electrolyte anodization process was used at varying anodization potential and time. At lower potential, no current flow and/or nanopores were seen even after 24hr of anodization time. However, by increasing the potential to 60V at a sweep rate of 50mV/s, the field generated was sufficient to form nanotubes (64.11 ± 2.7 nm) with enormous improvement in average surface roughness. The surface was hydrophilic to cell material and promising bioactivity as attested by good bone-forming ability after 28 days of immersion in simulated body fluid (SBF). It can be concluded that, desired surface aimed at enhancing the bioactivity of low modulus Ti alloy can be achieved under suitable anodization conditions.

Keywords: *Surface roughness, Bioactivity, Anodization, Anodization parameter*

1. INTRODUCTION

Bioactivity defines the degree to which a biomaterial affects, interacts with, or triggers response from living tissue. Higher bioactivity indicates more biochemical pathways for enhanced tissue/implant communication. This favours effective implant-host union via bone ingrowth into the implant (osseointegration) or around the bone (peri-implant trabecula bone), the two structural components of implant-host assembly [1-4]. As a gateway for implant-host communication, the material's surface needs to be reactive. In other words, the material must allow some bio-chemical activities for firm attachment at least on the surface. However, Ti-alloys are known for high corrosion resistance; in fact, this has been one of their comparative advantages as materials of choice in the field of biomaterials. This comes with poor bonding ability (somehow bioinert to the neighbouring tissues) and bone material cannot infiltrate to stimulate the initialization of bone apposition after implantation [5-6].

Osseointegration (bone ingrowth in an implant) is catalyzed by the degree of surface roughness, hence moderately rough surface is advantageous for effective implant-cell union. In fact, the rougher the surface, the more biological responses it triggers [7]. By way of roughening the surface, Ti-alloys are made so bioactive that they mimic the natural bone at least at the implant-host interfaces [2,8].

Bioactive coatings like hydroxyapatite (HAp) are widely used to achieve suitable roughness for implant-joint union. drawbacks like delamination and distortions usually occurs as coatings differ with both the implant and the adjoining host. This results in premature failure and in some case with adverse cytotoxic reactions [2].

Consequently, developing nanostructured oxide films on titanium alloy surfaces (nanopores) is considered as an effective way of achieving sound interaction with neighbouring tissues. This is due to their biocompatibility as they display superior wettability, sufficient corrosion resistance, and enhanced catalytic and biological properties and they are part of the parent implant (i.e. no junction) [3, 9-12]. It also operate as a transition region which bridges modulus mismatch at both ends (substrate and tissue), thus Titanium Nanotubes (TNTs) can also be employed to lower elastic modulus to as close as that of bone for effective load transfer [13].

Nanopores can be created by hydrothermal methods, plasma electrolytic oxidation, or electrochemical oxidation (anodization). Among these techniques, anodization gains universal acceptance as it is simple, flexible, time and cost-effective [3], environmentally friendly [14], and produces uniform and reproducible nanostructured oxide films (TiO_2) on titanium alloys [15]. In line with this, anodization is considered suitable for the development of nanotubes to allow for enhanced osseointegration.

1.1. Anodization

Anodization is regarded as growth of a controlled oxide film on a metallic component which form anode in an electrochemical cell. Anodization follows the fundamentals of electrolysis. This is to say, pores can be fine-tuned in the light of thickness, size, topography, and chemistry by controlling anodization potential, time, electrolyte, and alloying elements. Anodization promotes the creation of tubular nanostructure on the surface of Ti and its alloys (Figure 1); and this presents higher oxidation degree, surface energy, as well as considerable improvement in biocompatibility [16]. It also improves vital characteristics (like wear resistance) which are key to dental and orthopaedic applications. More so, TiO_2 nanotubes provide room for an increased channelling and fluid exchange within and across the implant leading to better and speedy healing [5].

Fluoride and phosphate ions-based electrolytes are commonly used for Ti-alloys anodization. However, the former (F^- based) are preferred as they are much more smaller and have higher diffusion coefficient; hence the ions diffuse through the metal oxide and effectively grow the needed pores [17, 18]. Such growth in F^- based electrolyte involves three basic stages: Oxide formation, oxide dissolution and growth of nanotube development.

Stage I: Field assisted oxidation: here a dense oxide is formed (Fig.1a), an electric field generated upon application of voltage ionizes H_2O and TiO_2 is produced through the interaction of O^{2-} and Ti. This progresses swiftly as the anion diffuses across the metal oxide to reach the metal/oxide [M-O] interface and reacts with metal ions (Ti^{4+} cation) beneath the surface and form a dense oxide layer of TiO_2.

$$Ti + 2H_2O \rightarrow TiO_2 + 4H + 4e^- \quad (1)$$

Step II: Field assisted dissolution under the influence of an electric field, the Ti^{4+} cations formed migrate to oxide/electrolyte [O-E] interface via M-O interface and expelled into the electrolyte. This creates some pits (Fig. 1b) which grow to form porous oxide. On the other hand, TiO_2 oxides layer are continuously formed due to the migration of O^{2-} to M-O interface.

$$Ti^{4+} + 2O^{2-} \rightarrow TiO_2 \quad (2)$$

Step III: Tube development: F^-gradually etch the barrier into small pores (Fig. 1c). This chemical dissolution of TiO_2 progresses inward (Fig. 1d) until an equilibrium between dissolution rate of TiO_2 nanotubes on the top equals the growth rate of the nanotubes at M-O interface (Fig.1e) and the overall titanium nanotubes TNTs (Fig.1f) are formed in accordance with equation 3 [19-20].

$$TiO_2 + 6NH_4F \rightarrow TiF_6^{2-} + 6NH_3 + 2H_2O + 2H^+ \quad (3)$$

The nature (height, shape, and diameter) of pores produced are controlled by anodization potential [21], type and pH of the electrolyte [11][12], alloying elements [3] and anodization time [19].

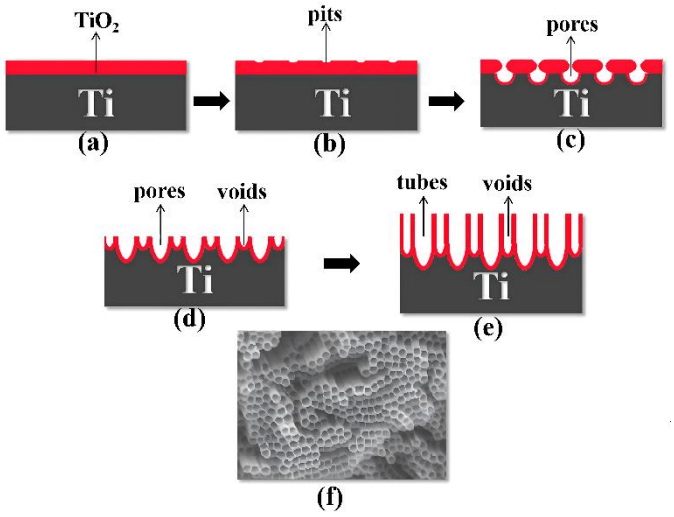

Figure 1. Schematic diagram of TNTs formation via anodization. Reproduced with permission [20].

The higher the voltage, the more spherical the pores become. However, the diameter of the pore increases with increasing potential [3]. Oxide films grow at 4 nm/V [10] and thicken at 2 – 3 nm/V [22]. Chen et al. [21] reported an increase in both pore length (458 nm, 546 nm, and 1 μm) and diameter (104 nm, 127 nm, and 191 nm) at respectively 50 V, 70 V, and 100 V potential. On the other hand, the use of considerably low potential (5 or 10 V) produces nanopores within the range of 30 – 40nm [16] and depending on alloying elements, β-phase (enriched with beta stabilizers) showed a smaller pore diameter (15 nm) as against α with 25 nm after anodization at 5 V. Similar phase-diameter relationship was reported by Buckner et al., [10]. On the other hand, anodization time dictates the overall volume of the nanotubes. Its effect is more pronounced on the tube length rather than the diameter.

Lee et al., [23] observed variation in both pore diameter and length (10 nm and 100 nm); (15 nm and 200 nm); (20 nm and 250 nm) and (35 nm and 300 nm) at 10V for respectively 2, 5, 10 and 20 minutes.

Bioactivity is a function of pores diameter, for instance, micropores of 50–150 μm diameter allow vascularization and migration of stem cells as well as osteo-inductive cues. However, pores of smaller diameters offer higher adhesion of osteoblasts and thus are preferred for enhanced bioactivity [5, 24]. It is against this background that the present study seeks to vary anodization parameter(s) and produce suitable TNTs for enhanced alloy's bioactivity.

2. MATERIALS AND METHODS

2.1. Sample Preparation

The beta type Ti-13Mo-2Fe alloy developed in our previous study [25] was sectioned and mounted in an epoxy resin while attaching a copper wire to the sample for an electrical connection. This ensured that only the intended surface is anodized.

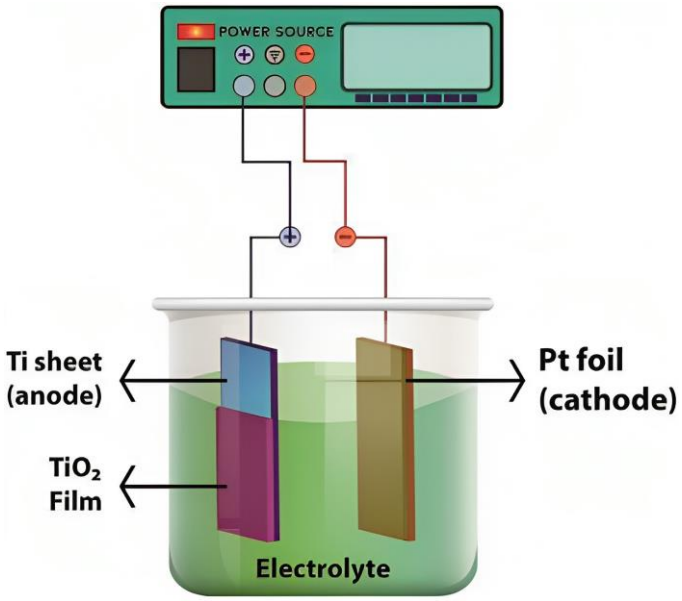

Figure 2. Setup for two electrodes anodization process [19].

As shown in Figure 2, the anodization process employed the use of two-electrodes (anode and cathode) connected to a potentiostat (PARSTAT 4000) operated with Versa Studio software. The anode (substrate) and the cathode (platinum rod) were placed ~3 cm away from each other in a fluoride-based electrolyte.

The choice of fluoride-containing organic electrolytes is based on its suitability to forming porous anodic films on titanium and its alloy. As against non-fluorine-based electrolytes (like $NaClO_4$ + NaCl + H_2O + C_2H_5OH; NaCl + H_2O + glycerol; KBr + H_2O + glycerol; $HClO_4$ + $NaClO_4$ etc), fluorine-based electrolyte owns a reputation of forming nanotubes of uniform size and thickness [12]. More so, fluoride ions have significantly high diffusion coefficients and smaller Van der Waals radius among number of electrolytes [17] and is widely associated with the formation of self-assembled nanotubes [19, 26]. In fact, it is very effective when anodizing Fe containing Ti-alloys [18]. Consequently, 0.5g NH_4F (Sigma-Aldrich reagent grades) + 5ml of deionized (DI) H_2O in 95 ml ethylene glycol ($C_2H_6O_2$) was prepared. The electrolyte was mixed for 10 minutes with a magnetic stirrer at 300 rpm.

2.1. Anodization Process

The anodization progresses at varying potential (10, 20, 30, 40, 50 and 60 V) for varying time; however, only 60 V recorded a flow of current in the range of 0.001 A. Consequently, 60V swept at 50 mV/s was used as anodization potential. Meanwhile, anodization time was varied until a clear nanotube were achieved. The choice of low sweep voltage was to ensure uniformity in the tube thickness being grown. At the end of anodization, the samples were carefully cleaned off debris while reducing the content of fluoride ions (F^-) using ethanol. The remaining fluoride ions (F^-) are eliminated by annealing as they cause instability and ions migration at both film/electrolyte and metal/film interfaces. This continued electrochemical process represents material degradation by way of pitting corrosion. More so, fluoride ions increases the risk of peeling and cracking of the TNTs [19], and discourages cellular activities [27-28] thus, must be eliminated for biocompatibility. Consequently, the samples were annealed at 400 °C 2 ˚ min^{-1}, for 3 hr in line with other studies success. This is to ensure not only fluoride ions removal but avoidance collapse or deterioration of nanotubes by way of converting the as-anodized

(amorphous) into more bioactive, biocompatible and high-strength crystalline TNTs [14, 16, 29, 30].

3. CHARACTERIZATION

Field Emission Scanning Electron Microscope (FESEM-Supra 35VP, Zeiss - Germany) was used to inspect the formation of pores as function of V and time. Atomic Force Microscope (AFM-SPA400) was used to study the degree of roughness while alloy's wettability was assessed by measuring the water contact angle using (Ossia goniometer). More so, apatite formation after 28 days of immersion in simulated body fluid (SBF) was used to assess the sample's bioactivity.

3.1. Determination of Surface Roughness

Surface topography play a vital role in the behaviour of biomaterials as well as implant-host interaction. Consequently, an Atomic Force Microscope (AFM) was used to assess the surface characteristics of the alloy. Surfaces of polished, anodized, and annealed samples were examined with AFM (SPA400) equipped with 20 μm scanner and operated via NanoNavi software. True 3-D surface profile, surface roughness and the thickness of the tubes were visualized. To have a good representation of surface topography, a projected area of 25 μm^2 at five different places were scanned from which an average roughness (Ra) was calculated using Gwyddion software.

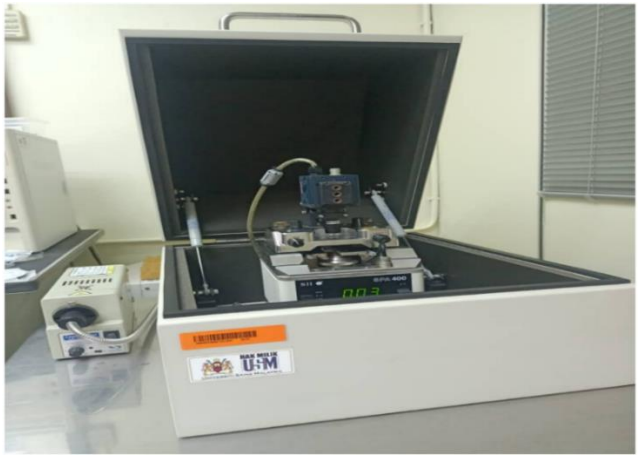

Figure 3. Image of Atomic Force Microscope AFM-SPA400.

3.2. Contact Angle Measurement

A contact-angle goniometer (Ossia) was used to measure the contact angle using a controlled drop of de-ionized (DI) water through a micro pipette. The spread was recorded within 2 s of dropping the DI water. For consistency, three drops on different areas of each sample were considered.

3.3. Evaluation for Hydroxyapatite Growth

Being a function of biological response of a material, the formation of apatite is widely used to predict a material's biological activity [31-33]. In vivo bone bioactivity and/or mineralization abilities was assessed by immersing a biomaterial in a simulated body fluid (SBF). SBF provide an approximate replica of the blood tissue environment in laboratory conditions, such that the ions (Ca and P) constituting SBF adsorb and permeate into porous TiO_2 form apatite [14, 34]. The SBF was prepared in line with Kokubo standard procedure while the minimum volume of SBF required in relation to sample size was determined usign equation (4). A pH meter (Eutech Instruments pH 510) was used to monitor the pH while adding tris (tris (hydroxymethyl)aminomethane) and any rise above 7.45 was countered by adding hydrochloric acid (HCl) [35]. To maintain ion concentration, the solution was refreshed every two days while samples were removed from the BSF and assessed after 28 days of immersion. The bioactivity was evaluated by examining hydroxyapatite formation on the nanotube layers after soaking in SBF at 36.57 ± 1.5 1 ^{o}C for 28 days.

$$V_s = \frac{S_a}{10} \quad (4)$$

Where S_a is the total surface area (ie sum of curved surface area and circular bases), r = radius of the sample, t = thickness of the sample:

$$S_a = 2\pi r^2 + 2\pi rt \quad (5)$$

4. RESULTS AND DISCUSSION

The FESEM images of sample anodized under various conditions showed no defined nanotubes (Figure 4) at a potential of 10 V, 20 V and 30 V. More so, there were no flow of current (in the range of 0.001 A) even after 24 hr of anodization time and the use of HF-H_2SO_4 based electrolyte.

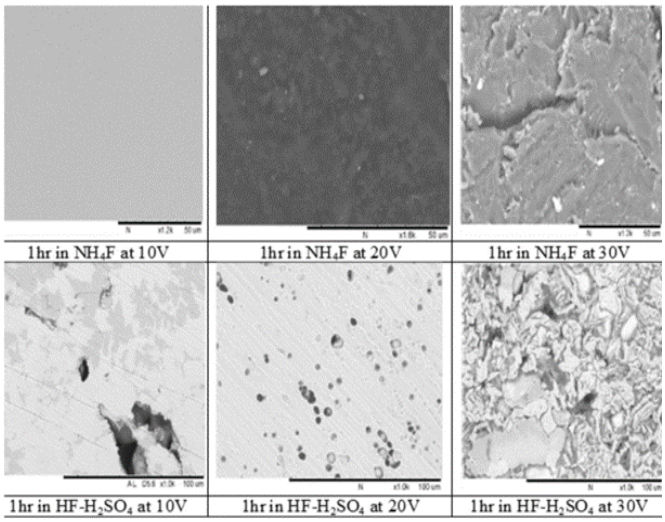

Figure 4. Anodized Ti-13Mo-2Fe in NH_4F and HF-H_2SO_4 based electrolytes at varying potentials.

Increasing the potential to ≥ 60 V, the nanotubes can be seen; however, at 15 minutes of anodization time, the pores are only partially revealed (Figure 5 A and B). By increasing the anodization time to 30 minutes, the tubes became well-defined (Figure 5 C and D). With the help of Image J software, the diameter of the pores was estimated from an average of 30 tubes. Consequently, the diameter of the tube was found to be 64.11 ± 2.7 nm. Souza et al., [15] postulate that a pore diameter below 120 nm enhances bioactivity. Nonetheless, relatively smaller diameter (around 50 nm) are required to induce cell activity, cell growth and differentiation [34, 35]. Other studies saw no variation in cell adhesion at between 30 to 70 nm pore diameter [36] and 30 to 87 nm [37]. However, cell attachment declined when the pore diameter exceed 87 nm. Mu et al., [37] inferred that nanotubes of about 70 nm diameter are most suitable for osteoconductivity, cell proliferation and differentiation while Li et al., [38] suggested a slightly above 70 nm to avoid excessive overcrowding.

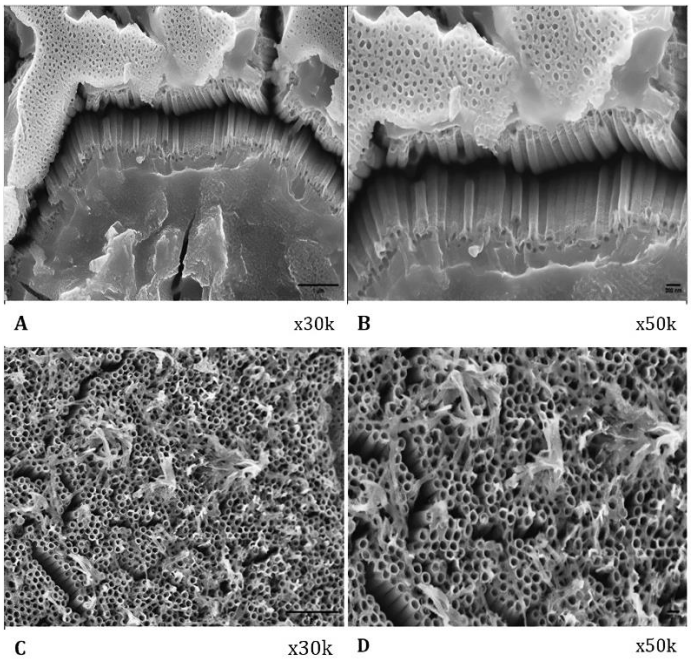

Figure 5. FESEM images showing surface morphology of samples anodized at 60V at 50mV/s at varying anodizing time: A) & B) 15 minutes. C) and D) 30 minutes.

In line with the aforementioned pore diameter-bioactivity relationship, the pore diameter of the TNTs (64.11 ± 2.7 nm) may be adequate for effective mineralization, cell attachment, proliferation, and growth. Consequently the Ti-13Mo-2Fe anodized at a sweep potential of 50mV/s to 60V for 30 minute is deemed promising in the light of bioactivity.

4.1. Surface Characterization

The parameters tested are average surface roughness (Ra), surface topography and contact angle (C.A). Figure 6 showed Ra and C.A while surface topography is shown in Figure 7. The average surface roughness (Ra) increases

from 18.74 ± 1.29 nm to 92.13 ± 4.43 nm (anodized) and slightly reduces to 71.06 ± 6.98 nm upon annealing.

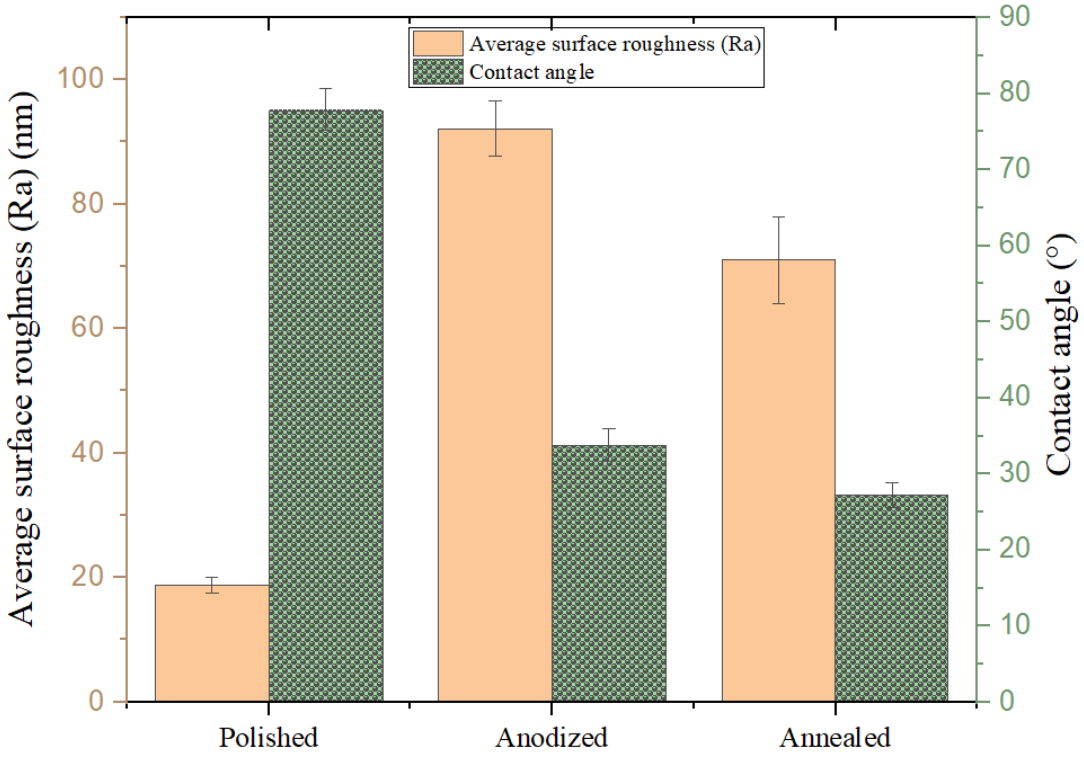

Figure 6. Surface properties under varying condition and treatment.

Such diminishing roughness due to annealing was reported with no significant variation due to calcination temperatures by Yu et al., [39]. The overall roughness can be considered adequate as oxides of moderate roughness (~68 nm) were reported to promote apatite formation in Ti-alloy [12].

As for the contact angle, it is worth knowing that a C.A below 90° implies hydrophilicity while above 90° implies hydrophobicity. In other words, lower C.A implies increased wettability and hence better attachment [36,40]. Additionally, studies have it that lower C.A.s (< 62°) provides the needed hydrophilicity for sound cellular response [7]. The respective values of CA are 77.92 ± 2.7°, 33.81 ± 2.2°, and 30.17 ± 4.2° for polished, anodized, and annealed samples. In other words, the annealed samples showed the highest wettability followed by anodized while polished has the least wettability. The result agrees with the findings of A et al., [14] where C.A reduced from 67° (for substrate) to 23° and 36° (for anodized samples); Khaw et al., [34] reported a significant reduction in C.A as a function of anodization. More so, the result surpasses the needed C.A for hydrophilicity which lead to an effective and favourable cellular response [7].

The 3-D surface topography attested the relatively highest Ra of anodized specimen (Figure 7b) while polished (Figure 7a) has the lowest roughness and intermediate roughness for the anodized and annealed sample. This signifies that anodization increases roughness of specimen and this reinforced the outcomes of contact angle as well as average surface roughness.

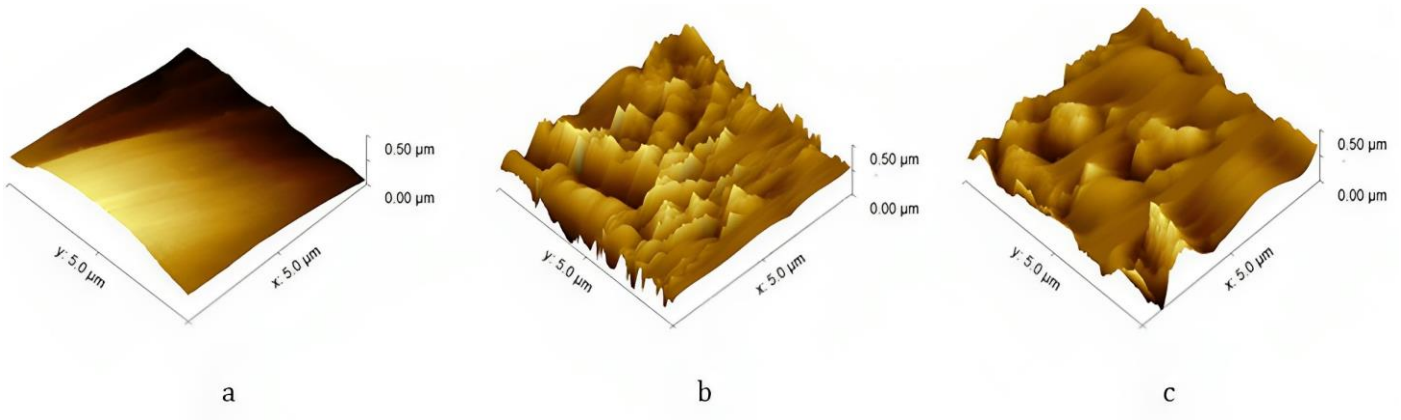

Figure 7. 3D surface view under different conditions and treatment: a) as polished b) anodized c) anodized and annealed.

4.2 Hydroxyapatite Growth

The micrograph (Figure 8) after 28 days of immersion in SBF revealed a well-grown appetite on the surface. This can be attributed to the surface topography which plays a vital role in the behaviour of biomaterials as well as implant-host interaction. Thus, the increased roughness which brought higher wettability is believed to have triggered the biological response. Generally speaking, rough surface encourage apatite grows by increasing surface adhesion thereby retaining and channeling the apatite formers [35]. This is believed to bring some stability around the SBF interface. Such stabilities are fundamental to apatite nucleation as various ions interact (micro- and nano-scale to) to form a nucleation site and bond produce the surfaces [37]. More so, apatite nucleation and growth is catalyzed when a biomaterial is "waterlogged" [38]. Additionally, the result of energy dispersive X-ray spectroscopy (EDS) showed the presence of P, O and Ca which are the basic elements in bone like apatite.

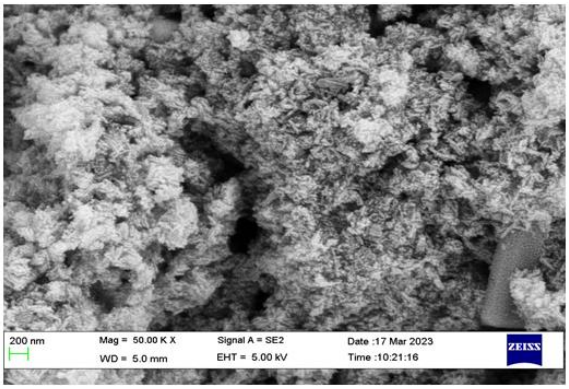

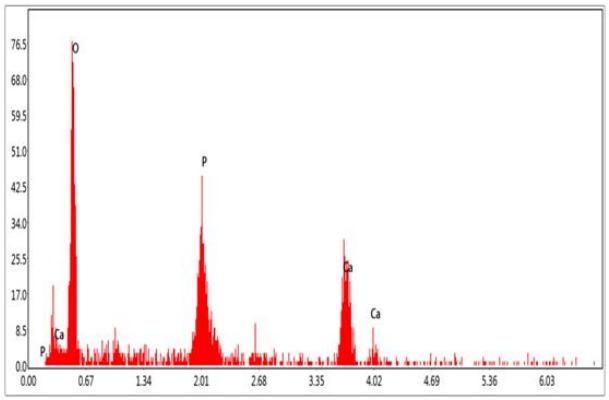

Element	Weight %	Atom %	Error %
O	38.76	50.08	14.41
P	20.51	16.14	8.06
Ca	40.73	24.78	9.19

Figure 8. Appetite formation on anodized Ti-13Mo-2Fe after 28 days of immersion is SBF.

5. CONCLUSION

By way of developing nanotubes, anodization has been demonstrated as an effective way of increasing surface roughness. The pore characteristics are fine-tuned by adjusting anodization potential and/or time. Increasing the potential to ≥ 60 V resulted in tube formation. However, clear TNTs were only seen after 30 minutes of anodization. This confers a promising bioactivity to the alloy as improved wettability and appetite forming ability was demonstrated. Consequently, anodization at sweep potential of 50 mV/s to 60 V for 30 minutes is considered adequate for mineralization and bioactivity.

ACKNOWLEDGMENTS

This work is supported by Ministry of Higher Education Malaysia for Fundamental Research Grant Scheme with Project Code FRGS/1/2018/TK05/USM/01/5 and for the first author is financially supported by Tertiary Education Trust Fund (TETFund), Nigeria under Academic Staff Training and Development Scheme with Reference Code TETF/ES/POLY/KATSINA/TSAS/2018/VOL.I.

REFERENCES

[1] Escada A. L., Nakazato R. Z., and Claro A. P. R. A., 'Influence of anodization parameters in the TiO2 nanotubes formation on Ti-7.5Mo alloy surface for biomedical application', *Mater. Res.*, vol. 20, no. 5, pp. 1282–1290, 2017, doi: 10.1590/1980-5373-MR-2016-0520.

[2] M. Jarosz, J. Grudzień, J. Kapusta-Kołodziej, A. Chudecka, M. Sołtys, and G. D. Sulka, *Anodization of titanium alloys for biomedical applications*. 2020.

[3] M. Jarosz, L. Zaraska, M. Kozieł, W. Simka, and G. D. Sulka, 'Electrochemical oxidation of Ti15Mo alloy—the impact of anodization parameters on surface morphology of nanostructured oxide layers', *Nanomaterials*, vol. 11, no. 1, pp. 1–14, 2021, doi: 10.3390/nano11010068.

[4] F. Les, G. Cásedas, and V. López, 'Bioactivity of medicinal plants and extracts', *Biology (Basel).*, vol. 10, no. 7, pp. 11–12, 2021, doi: 10.3390/biology10070634.

[5] L. Mohan, C. Anandan, and N. Rajendran, 'Electrochemical behavior and effect of heat treatment on morphology, crystalline structure of self-organized TiO2 nanotube arrays on Ti–6Al–7Nb for biomedical applications', *Mater. Sci. Eng. C*, vol. 50, pp. 394–401, 2015, doi: 10.1016/j.msec.2015.02.013.

[6] A. Jaafar, C. Schimpf, M. Mandel, C. Hecker, D. Rafaja, L. Krüger, P. Arki, Y. Joseph., 'Sol–gel derived hydroxyapatite coating on titanium implants: Optimization of sol–gel process and engineering the interface', *J. Mater. Res.*, vol. 37, no. 16, pp. 2558–2570, 2022, doi: 10.1557/s43578-022-00550-0.

[7] Q. Wang, P. Zhou, S. Liu, S. Attarilar, R. Ma, Y. Zhong, L. Wang, 'Multi-scale surface treatments of titanium implants for rapid osseointegration: A review', *Nanomaterials*, vol. 10, no. 6, pp. 1–27, 2020, doi: 10.3390/nano10061244.

[8] M. Saini, Y. Singh, P. Arora, V. Arora, and K. Jain, 'Implant biomaterials: A comprehensive review', *World J. Clin. Cases*, vol. 3, no. 1, pp. 52–57, 2015, doi: 10.12998/wjcc.v3.i1.52.

[9] H. J. Haugen and S. P. Lyngstadaas, *Antibacterial effects of titanium dioxide in wounds*, vol. 2. Elsevier Ltd, 2016.

[10] Dergin, G., Emes, Y., & Yusuf, B. (2016). Evaluation and Management of Mandibular Fracture. *Trauma in Dentistry*, *11*, 13. https://doi.org/doi.org/10.5772/intechopen.83024.

[11] M. İzmir and B. Ercan, 'Anodization of titanium alloys for orthopedic applications', *Front. Chem. Sci. Eng.*, vol. 13, no. 1, pp. 28–45, 2018, doi: 10.1007/s11705-018-1759-y.

[12] M. R. Siti Nur Hazwani, L. X. Lim, Z. Lockman, and H. Zuhailawati, 'Fabrication of titanium-based alloys with bioactive surface oxide layer as biomedical implants: Opportunity and challenges', *Trans. Nonferrous Met. Soc. China (English Ed.*, vol. 32, no. 1, pp. 1–44, 2022, doi: 10.1016/S1003-6326(21)65776-X.

[13] B. Voltrova, P. Jarolimova, V. Hybasek, V. H. Blahnova, J. Sepitka, V. Sovkova, R. Matejka, M. Daniel, J. Fojt, E. Filova, 'In vitro evaluation of a novel nanostructured Ti-36Nb-6Ta alloy for orthopedic applications', *Nanomedicine*, vol. 15, no. 19, pp. 1843–1859, 2020, doi: 10.2217/nnm-2020-0123.

[14] S. A, S. V. G. A, M. Narayanan, N. N, and R. Nagumothu, 'Effect of electrolyte composition and heat treatment on corrosion resistance of coatings developed on Cp-Ti by anodisation', *Adv. Mater. Process. Technol.*, vol. 00, no. 00, pp. 1–11, 2020, doi: 10.1080/2374068X.2020.1855961.

[15] M. R. D. Souza, N. T. C. Oliveira, N. K. Kuromoto, and C. E. B. Marino, 'Growth and electrochemical stability of self-organized TiO 2 nanotubes on Ti-2 grade and orthopedic Ti6Al4V alloy for biomedical application', pp. 53–60, 2014.

[16] T. M. David, P. R. Dev, P. Wilson, P. Sagayaraj, and T. Mathews, 'A critical review on the variations in anodization parameters toward microstructural formation of TiO 2 nanotubes', *Electrochem. Sci. Adv.*, vol. 2, no. 4, pp. 1–64, 2022, doi: 10.1002/elsa.202100083.

[17] A. L. R. Rangel, G. R. Moreira Santos, and A. P. Rosifini Alves Claro, 'Nanotubes growth on Ti-15Mo alloys by anodization at low voltage', *Mater. Sci. Forum*, vol. 869, pp. 924–929, 2016, doi: 10.4028/www.scientific.net/MSF.869.924.

[18] S. Chen, Y. Ni, J. Zhang, Y. Dan, W. Zhang, Y. Song, and X. Zhu., 'Double-anode anodization of metal Ti in two beakers', *Electrochem. commun.*, vol. 125, p. 106991, 2021, doi: 10.1016/j.elecom.2021.106991.

[19] P. Bocchetta, L. Y. Chen, J. D. C. Tardelli, A. C. Dos Reis, F. Almeraya-Calderón, and P. Leo, 'Passive layers and corrosion resistance of biomedical Ti-6Al-4V and β-Ti alloys', *Coatings*, vol. 11, no. 5, pp. 1–32, 2021, doi: 10.3390/coatings11050487.

[20] W.-J. Lee, M. Alhoshan, and W. H. Smyrl, 'Titanium Dioxide Nanotube Arrays Fabricated by Anodizing Processes', *J. Electrochem. Soc.*, vol. 153, no. 11, p. B499, 2006, doi: 10.1149/1.2347098.

[21] D. Wähnert, J. Greiner, S. Brianza, C. Kaltschmidt, T. Vordemvenne, and B. Kaltschmidt, 'Strategies to Improve Bone Healing: Innovative Surgical Implants Meet Nano-/Micro-Topography of Bone Scaffolds', *Biomedicines*, vol. 9, no. 7, pp. 1–20, 2021, doi: 10.3390/biomedicines9070746.

[22] T. T. Bashir, H. Zuhailawati, and M. A. H. Gepreel, 'Evaluation of hardness and elasticity of thermo-mechanically processed low modulus Ti alloys for dental application', *Mater. Today Proc.*, vol. 66, pp. 2856–2861, 2022, doi: 10.1016/j.matpr.2022.06.529.

[23] E. Krasicka-Cydzik, 'Anodic Layer Formation on Titanium and Its Alloys for Biomedical Applications', *Titan. Alloy. - Towar. Achiev. Enhanc. Prop. Divers. Appl.*, 2012, doi: 10.5772/34395.

[24] A. Ahmad, Z. Ahmad, E. U. Haq, W. Akhtar, and M. Arshad, 'Synthesis and characterization of titania nanotubes by anodizing of titanium in fluoride containing electrolytes', *Appl. Nanosci.*, vol. 7, no. 8, pp. 701–710, 2017, doi: 10.1007/s13204-017-0608-5.

[25] K. Shahzad, E. Tsuji, Y. Aoki, S. Nagata, and H. Habazaki, 'Formation and field-assisted dissolution of anodic films on iron in fluoride-containing organic electrolyte', *Electrochim. Acta*, vol. 151, pp. 363–369, 2015, doi: 10.1016/j.electacta.2014.10.132.

[26] J. G. Adams, 'PAEDIATRIC OVERDOSES', in *Emergency Medicine: Expert Consult*, Second., E. S. N. Erik D. Barton, Jamie Collings, Peter M. DeBlieux, Michael A. Gisondi, Ed. Elsevier Health Sciences, 2013, p. 1345.

[27] A. Strunecka and O. Strunecky, 'Mechanisms of fluoride toxicity: From enzymes to underlying integrative networks', *Appl. Sci.*, vol. 10, no. 20, pp. 1–24, 2020, doi: 10.3390/app10207100.

[28] M. Sarraf, B. Nasiri-Tabrizi, C. H. Yeong, H. R. M. Hosseini, S. Saber-Samandari, W. J. Basirun, T. Tsuzuki, 'Mixed oxide nanotubes in nanomedicine: A dead-end or a bridge to the future?', *Ceram. Int.*, vol. 47, no. 3, pp. 2917–2948, 2021, doi: 10.1016/j.ceramint.2020.09.177.

[29] N. Bashirom, W. K. Tan, G. Kawamura, A. Matsuda, and Z. Lockman, 'Formation of self-organized ZrO2-TiO2 and ZrTiO4-TiO2 nanotube arrays by anodization of Ti-40Zr foil for Cr(VI) removal', *J. Mater. Res. Technol.*, no. Vi, 2022, doi: 10.1016/j.jmrt.2022.06.055.

[30] P. Prochor and Ż. A. Mierzejewska, 'Bioactivity of PEEK GRF30 and Ti6Al4V SLM in simulated body fluid and hank's balanced salt solution', *Materials (Basel).*, vol. 14, no. 8, 2021, doi: 10.3390/ma14082059.

[31] A. Pradityana, N. Husodo, R. H. Ash Shiddieqy, and F. S. Pamasa, 'Analysis of corrosion rate and surface characteristics in substitution bone implant material with corrosive media simulated body fluid (SBF)', *IOP Conf. Ser. Mater. Sci. Eng.*, vol. 1034, no. 1, p. 012155, 2021, doi: 10.1088/1757-899x/1034/1/012155.

[32] Y. Mori, N. Masahashi, and T. Aizawa, 'A Review of Anodized TiNbSn Alloys for Improvement in Layer Quality and Application to Orthopedic Implants', pp. 1–17, 2022.

[33] T. Kokubo and H. Takadama, 'How useful is SBF in predicting in vivo bone bioactivity?', *Biomaterials*, vol. 27, no. 15, pp. 2907–2915, 2006, doi: 10.1016/j.biomaterials.2006.01.017.

[34] J. S. Khaw, C. R. Bowen, and S. H. Cartmell, 'Effect of tio2 nanotube pore diameter on human mesenchymal stem cells and human osteoblasts', *Nanomaterials*, vol. 10, no. 11, pp. 1–17, 2020, doi: 10.3390/nano10112117.

[35] D. Wähnert, J. Greiner, S. Brianza, C. Kaltschmidt, T. Vordemvenne, and B. Kaltschmidt, 'Strategies to Improve Bone Healing: Innovative Surgical Implants Meet Nano-/Micro-Topography of Bone Scaffolds', *Biomedicines*, vol. 9, no. 7, pp. 1–20, 2021, doi: 10.3390/biomedicines9070746.

[36] W. Singhatanadgit, M. Toso, B. Pratheepsawangwong, A. Pimpin, and W. Srituravanich, 'Titanium dioxide nanotubes of defined diameter enhance mesenchymal stem cell proliferation via JNK- and ERK-dependent up-regulation of fibroblast growth factor-2 by T lymphocytes', *J. Biomater. Appl.*, vol. 33, no. 7, pp. 997–1010, 2019, doi: 10.1177/0885328218816565.

[37] P. Mu, Y. Li, Y. Zhang, Y. Yang, R. Hu, X. Zhao, A. Huang, R. Zhang, X. Liu, Q. Huang, and C. Lin., 'High-Throughput Screening of Rat Mesenchymal Stem Cell Behavior on Gradient TiO2 Nanotubes', *ACS Biomater. Sci. Eng.*, vol. 4, no. 8, pp. 2804–2814, 2018, doi: 10.1021/acsbiomaterials.8b00488.

[38] Y. Li, S. Wang, Y. Dong, P. Mu, Y. Yang, X. Liu, C. Lin, and Q. Huang, 'Effect of size and crystalline phase of TiO2 nanotubes on cell behaviors: A high throughput study using gradient TiO2 nanotubes', *Bioact. Mater.*, vol. 5, no. 4, pp. 1062–1070, 2020, doi: 10.1016/j.bioactmat.2020.07.005.

[39] W. Q. Yu, Y. L. Zhang, X. Q. Jiang, and F. Q. Zhang, 'In vitro behavior of MC3T3-E1 preosteoblast with different annealing temperature titania nanotubes', *Oral Dis.*, vol. 16, no. 7, pp. 624–630, 2010, doi: 10.1111/j.1601-0825.2009.01643.x.

[40] S. N. F. Khairudin, H. F. Pahroraji, S. K. Alias, and M. H. I. Ibrahim, 'A Review of Metal Injection Moulding on WC-Co Cemented Carbide Comprised of Grain Growth Inhibitors (GGI)', *Int. J. Integr. Eng.*, vol. 14, no. 1, pp. 84–101, 2022, doi: 10.30880/ijie.2022.14.01.009.